ASSESSMENT OF DEPTH-DISTRIBUTED FALLOUT RADIONUCLIDE (FRNS) AND SOIL EROSION/DEPOSITION IN THE HILLSLOPE DISTRICT (KHAGRACHARI) IN BANGLADESH

KHAN, M. R.[1] – TARAFDER, M. M. A.[1] – GABER, A.[2] – BAREK, V.[3] – BRESTIC, M.[4] – HOSSAIN, A.[5*]

[1]*Soil Science Division, Bangladesh Institute of Nuclear Agriculture, Mymensing, Bangladesh*
(e-mail: binamunna@yahoo.com – M. R. Khan; totunbina@yahoo.com – M. M. A. Tarafder)

[2]*Department of Biology, Faculty of Science, Taif University, P.O. Box 11099, 21944 Taif, Saudi Arabia*
(e-mail: a.gaber@tu.edu.sa)

[3]*Institute of Landscape Engineering, Faculty of Horticulture and Landscape Engineering, Slovak University of Agriculture Nitra, Tr. A. Hlinku 2, 94901 Nitra, Slovakia*
(e-mail: viliam.barek@uniag.sk)

[4]*Institute of Plant and Environmental Sciences, Slovak University of Agriculture Nitra, Tr. A. Hlinku 2, 94901 Nitra, Slovakia*
(e-mail: marian.brestic@uniag.sk)

[5]*Soil Science Division, Bangladesh Wheat and Maize Research Institute, Dinajpur 5200, Bangladesh*

**Corresponding author*
e-mail: akbarhossainwrc@gmail.com; phone: + 880-17-9004-9609

(Received 11th Jan 2025; accepted 19th Mar 2025)

Abstracts. This experiment was carried out on a hillside at the Hill Research Centre in the Khagrachari (23°8.509’ E, 092°00.059’ N) district to ascertain the erosion rate and depth distribution of a single fallout radionuclide (FRN) (^{137}Cs, ^{210}Pb, ^{210}Pbex, and ^{226}Ra) in 2020. Five locations, the summit, upper slope, middle slope, lower slope, and bottom, were used to gather the soil samples. A possible reference location was found 200 m away from the study area, with an elevation of 382 feet above mean sea level. The average value for ^{137}Cs in the local reference inventory was 946.4 Bq m^{-2}. The distribution of FRN (^{137}Cs, ^{210}Pb, ^{210}Pbex, and ^{226}Ra) tended to decrease as the soil depth increased. Compared with the reference inventory, the total inventory of the FRN at various sites revealed a similar trend from the summit to higher slope positions, indicating that these positions experienced soil erosion. The reference inventory was 144.5%, 108.1%, and 28.8% lower than the inventory for the bottom position (2314 Bq m^{-2}), lower slope position (1969.5 Bq m^{-2}), and medium slope position (1218.8 Bq m^{-2}), respectively. The soil eroded from the summit and upper slope positions by 24.93 and 6.33 t ha^{-1} yr^{-1}, respectively, and was deposited at the middle slope position (10.21 t ha^{-1} yr^{-1}), lower slope position (38.34 t ha^{-1} yr^{-1}), and bottom position (51.26 t ha^{-1} yr^{-1}). These estimated erosion/deposition rates were derived from mass balance Model II. The sediment delivery ratio was -219%, the gross erosion rate was 5.2 t ha^{-1} yr^{-1}, and the net erosion rate was 11.4 t ha^{-1} yr^{-1}. The entire inventory was 23.4% and 63.6% smaller than the reference inventory for the upper slope position (725.4 Bq m^{-2}) and the summit (344.5 Bq m^{-2}), respectively. The inventories were 28.8%, 108.1%, and 144.5% greater than the reference inventory for the intermediate slope position (1218.8 Bq m^{-2}), lower slope position (1969.5 Bq m^{-2}), and bottom position (2314 Bq m^{-2}), respectively, indicating that this site experienced soil sedimentation.

Keywords: FRN, soil redistribution erosion, depth distribution, deposition, hillslope,

Introduction

As a significant contributor to land deterioration, soil erosion presents a global threat to the environment and socioeconomic stability. It is exacerbated by overgrazing, poor agricultural practices, and climate change, especially on steep terrain (Blanco-Canqui and Lal, 2010). Reduced soil quality, fertility, productivity, and bioactivity put food security and soil ecosystem services at risk (Duan et al., 2011; Kumar et al., 2023). In line with this, it also exposes organic materials found in soil to oxidation, which raises the possibility of global warming (Van Oost and Six, 2023).

In the last 50 years, fallout radionuclides (FRNs: ^{137}Cs, ^{210}Pb, ^{226}Ra $^{210}Pb_{ex}$, and ^{7}Be) have been widely used as soil tracers to provide estimates of induced soil erosion rates under different environmental conditions (Ritchie and Ritchie, 2001; Zapata, 2002; Mabit et al., 2008). Once on the ground, FRNs travel over the landscape mostly by physical processes because of their high binding to tiny particles in surface soil (IAEA, 2014). As a result, the redistribution of soil and silt may be effectively tracked via these conservative radiotracers.

For arable lands, where soil degradation from agricultural practices influences soil characteristics and landscape processes, FRN approaches are effective in examining temporal soil redistribution patterns (IAEA, 2014). In mountain grasslands, where the harsh topography and climate make it difficult to use more traditional methods, such as sediment traps, erosion pins, or experiments with simulated rainfall, it is also very useful for evaluating patterns of erosion and deposition (Konz et al., 2012; Alewell et al., 2014). Different land uses can influence how soil is redistributed, resulting in erosion and/or deposition processes, which can also influence the siltation of natural and artificial water bodies (FAO, 2019).

The FRN method can be completed in a single sampling campaign and offers information on erosion processes that have affected a particular study area since the chosen FRN was deposited. This eliminates the need for time-consuming and expensive procedures that are typically needed to monitor sites over extended periods of time (Mabit et al., 2008, 2013). The technique is based on a targeted FRN comparison, which compares the inventory (total activity per unit area) at a sample location to that measured at a reference site that is nearby, undisturbed, and free of soil erosion and deposition.

When the rate of erosion of unploughed soils is estimated, the profile distribution models (PDMs) of Walling et al. (2011, 2014) are highly useful. The diffusion and migration model (DMM) and the mass balance model (MBM) consider the various vertical distributions of FRN in the soil on the basis of the migration processes following primary FRN deposition and the type of land use (ploughed or unploughed). Fallout radionuclides (FRNs) are frequently employed in studies on soil erosion (Zhang et al., 2006; Mabit et al., 2014a; Fulajtar et al., 2017). Nevertheless, a large body of research employing FRNs has concentrated on field size, with relatively few investigations and contrasting erosion rates calculated using both ^{137}Cs and $^{210}Pbex$ (Porto et al., 2016).

By comparing the ^{137}Cs inventories measured for individual sampling points with the reference inventory and using calibration models that relate the percentage loss or gain in the inventories to rates of soil loss or deposition, the study aims to estimate erosion and sedimentation rates. The reference inventory will be established through sampling of reference locations, comprehensive soil sampling to document the depth distribution of FRN (^{137}Cs, ^{210}Pb, ^{226}Ra, and $^{210}Pbex$), and total inventory.

http://www.aloki.hu ● ISSN 1589 1623 (Print) ● ISSN 1785 0037 (Online)
DOI: http://dx.doi.org/10.15666/aeer/2304_61616176

Materials and methods

Study site

At the Bangladesh Agricultural Research Institute's Hill Research Center in Khagrachari, Bangladesh (23°8.509' E, 092°00.059' N - 23°08.492' E, 092°00.047' N), a hill slope served as the study site (*Fig. 1*). The height above sea level is approximately 382 feet. The average annual temperature was recorded as 34.6°C, with a minimum of 13°C and an average rainfall of 3031 mm. The climate was categorized as semiarid continental monsoon.

Figure 1. *Experimental site*

Soil sampling

Soil samples were taken from five different locations on the hill: the summit (S), upper slope (US), middle slope (MS), lower slope (LS), and bottom (B) to ascertain the profile changes in the FRN (^{137}Cs, ^{210}Pb, ^{226}Ra, and ^{210}Pbex). The slope was 75 m wide by 60 m long. From each location, five sample points were chosen. An 8-cm diameter hand-operated core sampler was used to gather samples at 10- and 15-meter intervals along each transect of a hill slope and on terraces. At every sampling location, a single core was gathered and subsequently bulked to create a composite sample. To guarantee comprehensive FRN inventories of the soil profile, soil sampling depths were measured at the top (0–30 cm), upper and middle positions (0–45 cm), lower slope positions (0–60 cm), and bottom positions (0–100 cm with 5 cm increments).

When using ^{137}Cs data to estimate catchment erosion and sedimentation, the creation of a reference inventory is crucial. In response to these concerns, a prospective reference location with an elevation of 382 feet above mean sea level was found 200 m away from the research catchment (23°08.293' E, 91°59.815' N). Twelve cores, consisting of three replicate samples, were taken from a 10 × 10 square at depths ranging from 0 to 60 cm in 5 cm increments. The site, which is inside the study catchment, has little slope, no erosion or deposition, and it is completely covered with vegetation.

Analysis

The soil samples were weighed, allowed to air dry, and then sieved through a 2 mm screen. The amounts of ^{137}Cs, ^{210}Pb, ^{226}Ra, and ^{210}Pbex were determined via a

http://www.aloki.hu ● ISSN 1589 1623 (Print) ● ISSN 1785 0037 (Online)
DOI: http://dx.doi.org/10.15666/aeer/2304_61616176

multichannel analyzer connected to a hyperpure coaxial Ge detector. Using a counting duration of more than 80,000 s, the concentration of ^{137}Cs in the samples was found at 662 keV, yielding an analytical precision of ± 6% for ^{137}Cs. Mass balance Model 2 was used to calculate the rate of soil erosion–deposition (Walling and He, 1997).

Results

Depth redistribution of FRN (^{137}Cs, ^{210}Pb, ^{226}Ra and $^{210}Pb_{ex}$) at the reference site

The depth distributions of the ^{137}Cs activities and total inventories for the sampled reference profiles are shown in *Figure 2*. The ^{137}Cs activity of the reference populations decreased precipitously from 2.03 Bq kg^{-1} in the 0–5 cm layer to 0.52 Bq kg^{-1} in the 50–55 cm soil layer; no ^{137}Cs was detected in the 55–60 cm soil layer. The distribution of the ^{137}Cs probability with depth decreased to 55 cm; no ^{137}Cs activities were detected below this depth. The average value for the local reference inventory was 946.4 Bq m^{-2}. It is advised to compare these measurements made at the reference site with the location's projected global distribution value of ^{137}Cs.

Another notable decrease in ^{210}Pb activity was observed at 35–40 cm, ranging from 81.6 Bq kg^{-1} at 0–5 cm depth to 32.7 Bq kg^{-1}. ^{210}Pb had a total inventory of 33607.4 Bq m^{-2} at the reference inventory. The distribution of ^{226}Ra activity varied, ranging from 31.5 Bq kg^{-1} at 55-60 cm depth to 24.9 Bq kg^{-1} at 0-5 cm depth. At the reference site, the total inventory of ^{226}Ra was 33607.4 Bq m^{-2}. As the soil depth increased, the ^{210}Pbex activity decreased sharply, ranging from 56.64 Bq kg^{-1} at 0–5 cm to 5.6 Bq kg^{-1} at 35–40 cm. The overall inventory was 14417.0 Bq m^{-2}.

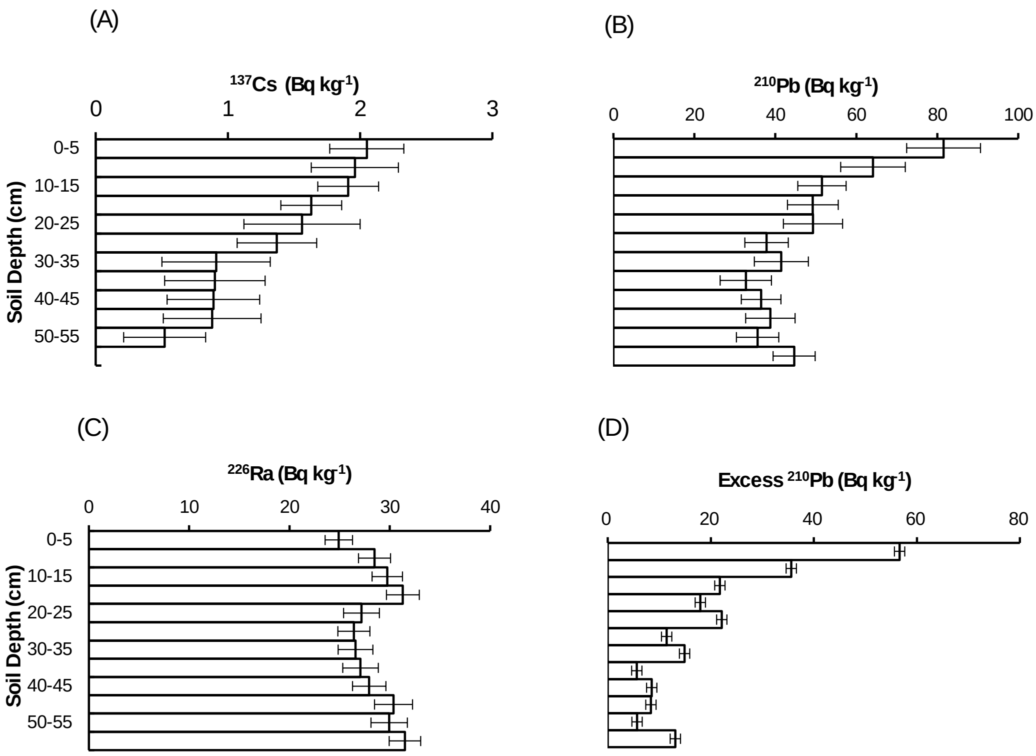

Figure 2. *Depth distributions of (A) ^{137}Cs, (B) ^{210}Pb, (C) ^{226}Ra and (D) $^{210}Pb_{ex}$ activity in undisturbed soil and reference sites. The error bar indicates the standard deviation (SD±), which was calculated from three replicates for each treatment*

http://www.aloki.hu ● ISSN 1589 1623 (Print) ● ISSN 1785 0037 (Online)
DOI: http://dx.doi.org/10.15666/aeer/2304_61616176

Quantifying the depth redistribution FRN (^{137}Cs, ^{210}Pb, ^{226}Ra and $^{210}Pb_{ex}$)

Cultivation is commonly used on terraced fields in steeply sloping areas when alternative approaches are not suitable for measuring erosion. Since the height, width, and length of terraces influence soil erosion, there is no trustworthy formula for determining the slope of terraced fields. ^{210}Pb, ^{226}Ra, ^{210}Pbex, and ^{137}Cs were dispersed over the upper 0–30 cm at the summit position (*Fig. 3*) of the experimental site. In the summit position study areas, where most erosion was predicted to occur but no deposition occurred, the ^{137}Cs activity ranged from 1.72 ± 0.21 to 0.44 ± 0.21 Bq kg^{-1}, the ^{210}Pb activity ranged from 79.7 ± 8.59 to 42.51 ± 6.11 Bq kg^{-1}, the ^{226}Ra activity ranged from 28.39 ± 1.48 to 2.71 ± 1.37 Bq kg^{-1}, and the ^{210}Pbex activity ranged from 55.23 ± 8.68 to 13.38 ± 6.33 Bq kg^{-1}.

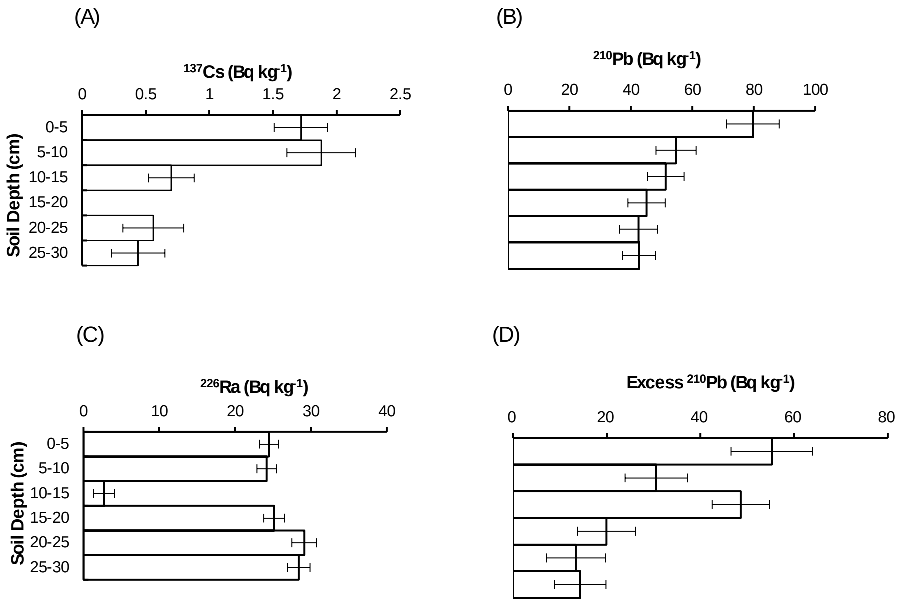

Figure 3. *Depth distributions of (A) ^{137}Cs, (B) ^{210}Pb, (C) ^{226}Ra and (D) $^{210}Pb_{ex}$ at the summit. The error bar indicates the standard deviation (SD±), which was calculated from three replicates for each treatment*

With respect to the higher slope position, ^{210}Pb, ^{226}Ra, and ^{210}Pbex were detected at depths of 0–45 cm, whereas ^{137}Cs was detected at depths of 0–40 cm (*Fig. 4*). In the studies conducted on the upper slope of the terraced areas, the ^{137}Cs activity ranged from 2.11 ± 0.26 to 0.87 ± 0.2 Bq kg^{-1}, the ^{210}Pb activity ranged from 76.83 ± 8.91 to 30.55 ± 5.29 Bq kg^{-1}, the ^{226}Ra activity ranged from 27.03 ± 1.39 to 24.27 ± 1.37 Bq kg^{-1}, and the ^{210}Pbex activity ranged from 51.53 ± 9.02 to 6.28 ± 5.46 Bq kg^{-1}. Because of human activity, this upper cultivated slope is considered a vulnerable area where soil erosion is prevalent.

Depending on the length and width of the slope location, the middle slope was taken into consideration for both soil deposition and erosion. The FRNs were dispersed across the upper 0–45 cm of the middle slope soil (*Fig. 5*). The ^{137}Cs activity varied from 4.19 ± 0.32 to 0.29 ± 0.15 Bq kg^{-1}, the ^{210}Pb activity ranged from 83.92 ± 9.6 to 35.77 ± 4.71 Bq kg^{-1}, the ^{226}Ra activity ranged from 28.77 ± 1.6 to 24.96 ± 1.27 Bq kg$^{-1,}$ and the ^{210}Pb$_{ex}$ activity ranged from 58.18 ± 9.7 to 7.86 ± 5.88 Bq kg^{-1} at the middle slope position of the study site.

http://www.aloki.hu ● ISSN 1589 1623 (Print) ● ISSN 1785 0037 (Online)
DOI: http://dx.doi.org/10.15666/aeer/2304_61616176

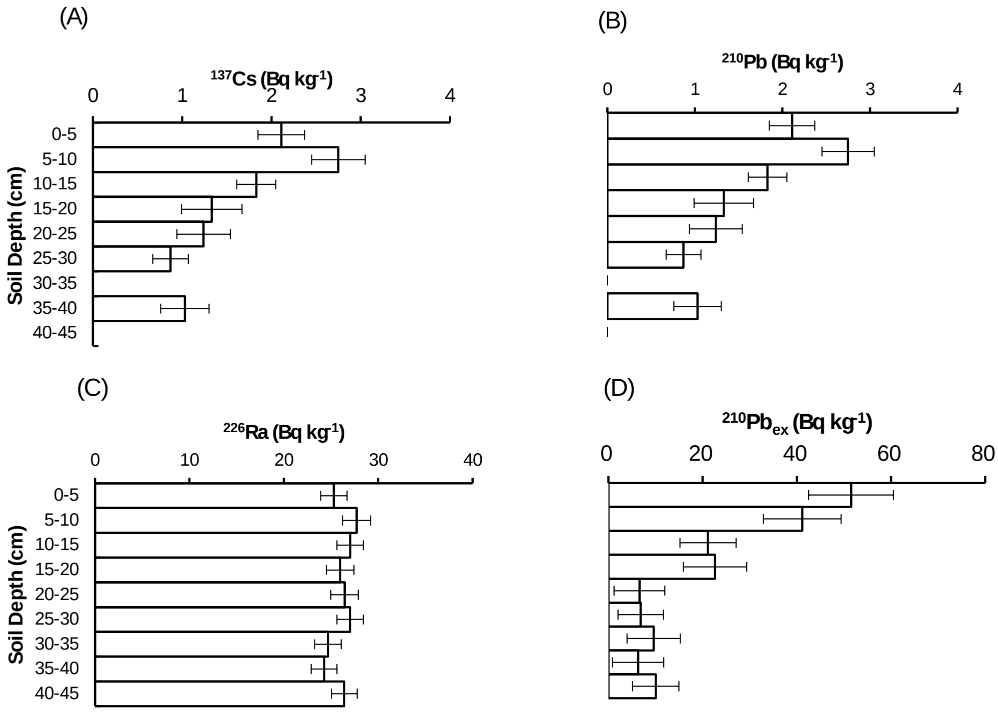

***Figure 4.** Depth distributions of (A) ^{137}Cs, (B) ^{210}Pb, (C) ^{226}Ra and (D) $^{210}Pb_{ex}$ at the upper slope position. The error bar indicates the standard deviation (SD±), which was calculated from three replicates for each treatment*

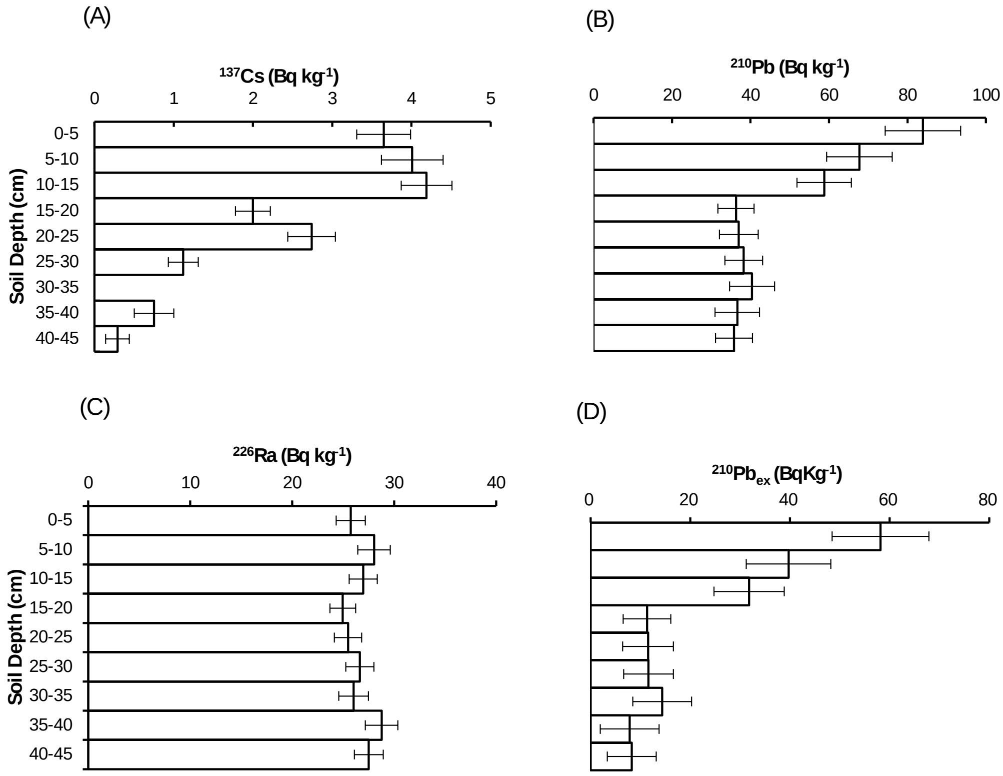

***Figure 5.** Depth distributions of (A) ^{137}Cs, (B) ^{210}Pb, (C) ^{226}Ra and (D) $^{210}Pb_{ex}$ at the middle slope position. The error bar indicates the standard deviation (SD±), which was calculated from three replicates for each treatment*

http://www.aloki.hu ● ISSN 1589 1623 (Print) ● ISSN 1785 0037 (Online)
DOI: http://dx.doi.org/10.15666/aeer/2304_61616176

The fallout radionuclide distributions were impacted by the lower slope position, which also had a substantially deeper layer of FRN throughout the time and cultivation period. Compared with the other slope sites, deeper soils presented greater FRN activity. FRNs were discovered in the upper 0–60 cm soil depth at lower slope positions (*Fig. 6*). At the lower position of the study site, the ^{137}Cs activity varied from 6.13 ± 0.38 to 0.39 ± 0.17 Bq kg^{-1}, the ^{210}Pb activity ranged from 88.66 ± 9.81 to 25.84 ± 4.08 Bq kg^{-1}, the + Ra activity ranged from 30.31 ± 1.65 to 25.4 ± 1.38 Bq kg^{-1}, and the ^{210}Pbex activity ranged from 60.02 ± 9.94 to 2.28 ± 4.14 Bq kg^{-1}.

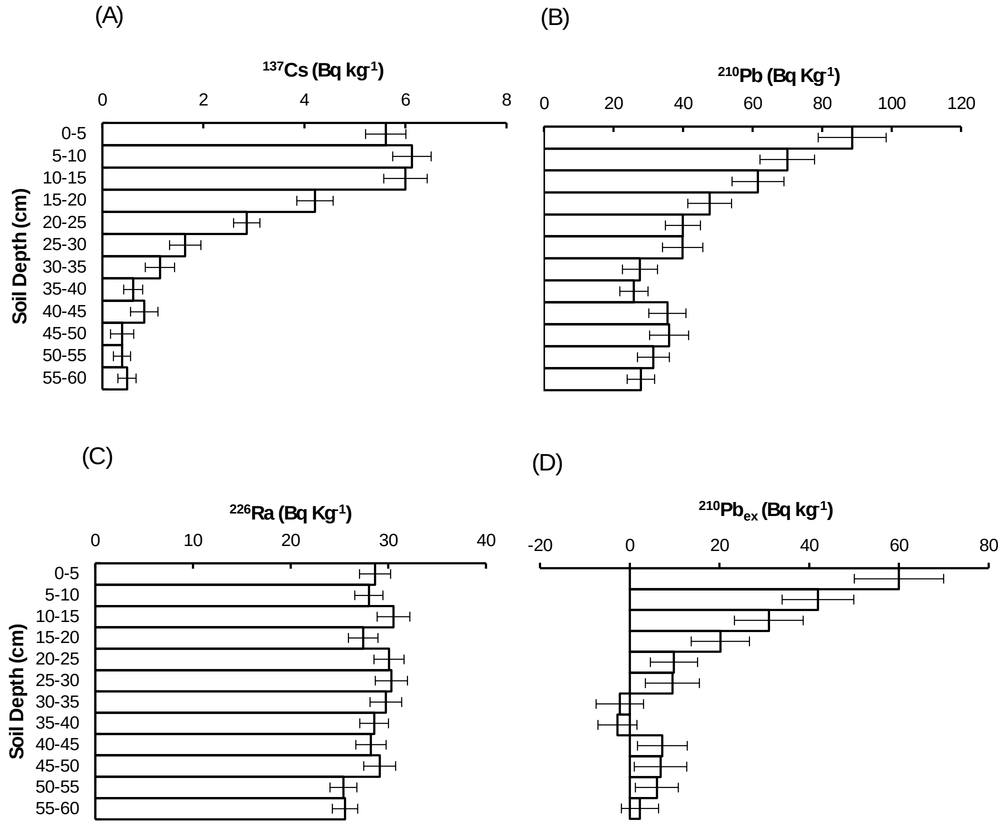

Figure 6. *Depth distributions of (A) ^{137}Cs, (B) ^{210}Pb, (C) ^{226}Ra and (D) ^{210}Pb$_{ex}$ at the lower slope position. The error bar indicates the standard deviation (SD±), which was calculated from three replicates for each treatment*

The slope position affected the fallout radionuclide distributions; in the lower position, FRN was present in a layer that was significantly deeper during the time and cultivation period, and the depth of FRN presence typically increased gradually. At the bottom position, ^{137}Cs was distributed in the top 0–70 cm, and ^{210}Pb, ^{226}Ra and ^{210}Pb$_{ex}$ were distributed in the 0–100 cm (*Fig. 7*). The ^{137}Cs activity varied from 4.82 ± 0.42 to 0.37 ± 0.17 Bq kg^{-1}, the ^{210}Pb activity ranged from 89.99 ± 2.91 to 26.95 ± 4.09 Bq kg^{-1}, the ^{226}Ra activity ranged from 28.87 ± 1.48 to 20.37 ± 1.21 Bq kg$^{-1,}$ and the ^{210}Pb$_{ex}$ activity ranged from 61.12 ± 3.26 to 2.19 ± 4.29 Bq kg^{-1} at the study site in the lower position.

Figure 8 displays the entire ^{137}Cs inventory of the reference site at various slope positions. The average values for the local reference ^{137}Cs, ^{210}Pb, ^{226}Ra, and ^{210}Pbex inventories were 946.4 Bq m^{-2}, 36607.4 Bq m^{-2}, 22190.4 Bq m^{-2}, and 14417 Bq m^{-2}, respectively.

http://www.aloki.hu ● ISSN 1589 1623 (Print) ● ISSN 1785 0037 (Online)
DOI: http://dx.doi.org/10.15666/aeer/2304_61616176

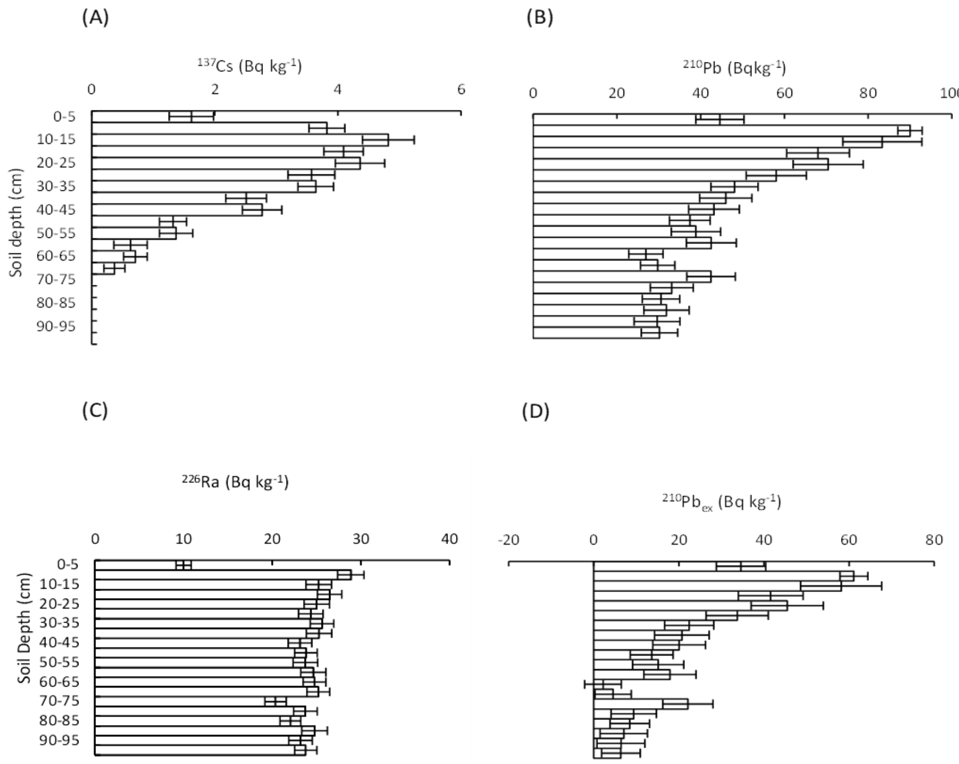

Figure 7. *Depth distributions of (A) ^{137}Cs, (B) ^{210}Pb, (C) ^{226}Ra and (D) ^{210}Pb$_{ex}$ at the bottom position. The error bar indicates the standard deviation (SD±), which was calculated from three replicates for each treatment*

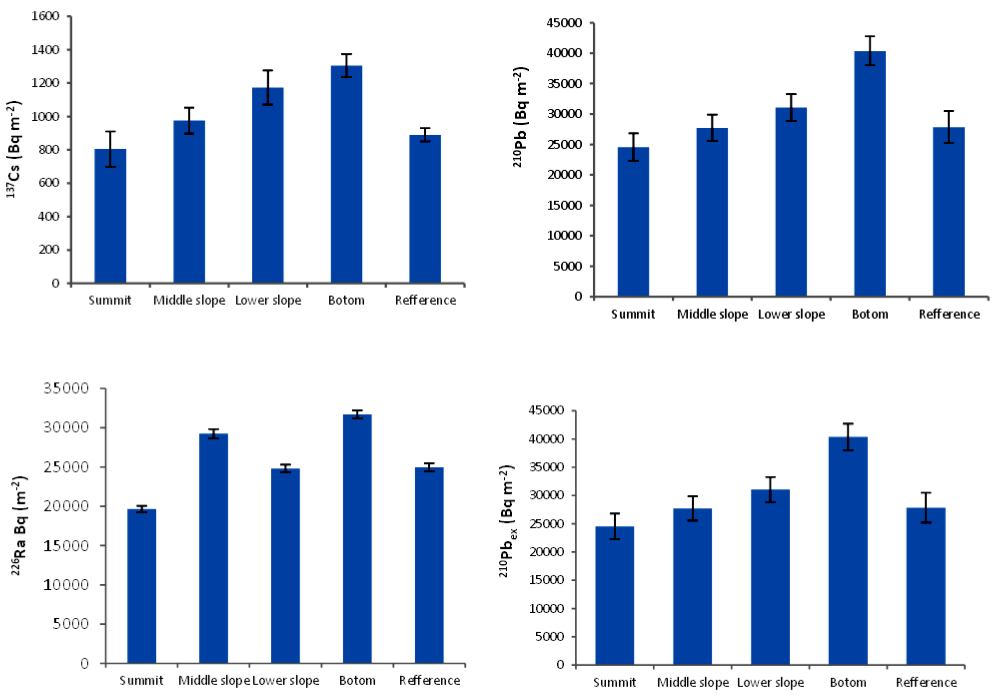

Figure 8. *Total FRN ((A) ^{137}Cs, (B) ^{210}Pb, (C) ^{226}Ra and (D) ^{210}Pb$_{ex}$) inventories (Bq m^{-2}) of the reference site and different slope positions. The error bar indicates the standard deviation (SD±), which was calculated from three replicates for each treatment*

http://www.aloki.hu ● ISSN 1589 1623 (Print) ● ISSN 1785 0037 (Online)
DOI: http://dx.doi.org/10.15666/aeer/2304_61616176

The entire inventory was 23.4% and 63.6% smaller than the reference inventory for the upper slope position (725.4 Bq m^{-2}) and the summit (344.5 Bq m^{-2}), respectively. This result suggested that soil erosion had occurred in these locations (*Fig. 9*). The reference inventory was 144.5%, 108.1%, and 28.8% lower than the inventory for the bottom position (2314 Bq m^{-2}), lower slope position (1969.5 Bq m^{-2}), and medium slope position (1218.8 Bq m^{-2}), respectively. Thus, soil sedimentation may have occurred at this position.

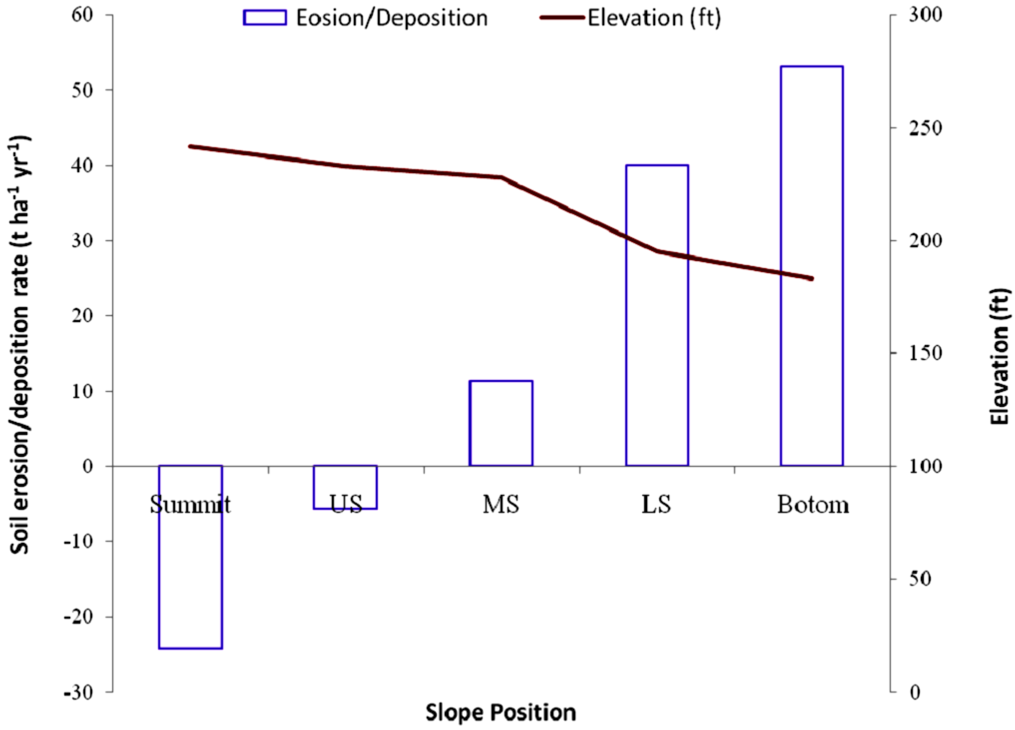

Figure 9. *Soil erosion (-ve) and deposition (+ve) rates at different slope positions and elevations*

To determine the rates of soil erosion and sedimentation associated with FRN stocks, mass balance models are available. The estimated erosion/deposition rates from mass balance Model II indicated that soil eroded from the summit and upper slope positions by 24.93 and 6.33 t ha^{-1} yr^{-1}, respectively, and was deposited at the middle slope position (10.21 t ha^{-1} yr^{-1}), lower slope position (38.34 t ha^{-1} yr^{-1}), and bottom position (51.26 t ha^{-1} yr^{-1}). Mass balance models have been used frequently to determine the spatial patterns of erosion and deposition rates. The sediment delivery ratio was -219%, the gross erosion rate was 5.2 t ha^{-1} yr^{-1}, and the net erosion rate was 11.4 t ha^{-1} yr^{-1}. The lower elevation received soil that had eroded from the higher level.

Discussion

Natural processes such as soil erosion and the ensuing soil redistribution caused by wind and water can be sped up by human activities such as overgrazing, mismanaged farms, land use changes, and deforestation. These processes not only result in offsite issues with sediment mobilization and transport as well as associated toxins that can

http://www.aloki.hu ● ISSN 1589 1623 (Print) ● ISSN 1785 0037 (Online)
DOI: http://dx.doi.org/10.15666/aeer/2304_61616176

enter dams, reservoirs, and water bodies but also generate onsite soil losses that impact crop yield (Dercon et al., 2006; Schmitter et al., 2010). In a different type of erosion known as tillage erosion, the gradual downslope movement of soil caused by tillage can result in soil loss and buildup in fields as well as worsening wind and water erosion (Dercon et al., 2007). Although soil erosion is the most common land degradation process in the world, emerging nations in Africa, Asia, and Latin America account for more than three-quarters of the total agricultural acreage damaged by erosion.

Measurement of ^{137}Cs

Gamma spectroscopy involves a specialized piece of equipment needed for the analysis of FRNs in soils and sediments. Its unique energy peak at a comparatively high energy level (662.66 KeV), which is unaffected by other radionuclides currently in use, makes measuring ^{137}Cs easier. As a result, it is simple to identify the concentration of ^{137}Cs isotopes in soil, which also makes it simple to use for studies on soil erosion. A high-purity germanium semiconductor detector (HPGe) with an amplifier connected to a multichannel analyser (MCA) and a computer with data evaluation software make up the Gamma Spectroscopic Analytical Set (Fulajtar et al., 2017).

Reference site

The depth distributions of FRN for the reference profile display higher concentrations at the surface and an approximately exponential decay distribution with depth (*Fig. 1*). By measuring the loss or accumulation of soil particles, the ^{137}Cs inventory in the soil can be used to quantify the soil erosion rate as the original fallout decreases due to radioactive decay. Because of this, a reference site with an undisturbed location with little to no erosion or sedimentation is needed for the measurement (IAEA, 2014; Walling and Quine, 1993). The FRN (^{137}Cs, ^{210}Pb, ^{226}Ra and $^{210}Pb_{ex}$) activities of the reference profiles declined sharply from the surface layer to the deeper layer to 55 cm, but the 55–60 cm depth of the soil did not contain FRN. An average value for ^{137}Cs of 946.4 Bq m^{-2} was found for the local reference inventory of the study area. Mandal et al. (2019) conducted a study in Dehradun, India, a neighboring country and reported ^{137}Cs values ranging from 944 to 1170 Bq m^{-2}. Tagami et al. (2019) conducted a study to assess the spatial distribution of ^{137}Cs reference site soils in South Asia and reported values ranging from 860 to 3731 Bq m^{-2}. The assessment of the erosion rate is based on the study of ^{137}Cs in the soil at reference and sample sites (Zhang et al., 2021). To the best of our knowledge, this paper provides the first study of soil erosion in hilly areas of Bangladesh using ^{137}Cs.

Depth distributions for different slopes

The numerous elements that influence soil erosion include soil type, long-term management/conservation techniques, rainfall amount and intensity, lithology, hill slope position, slope class, and land cover density. It is especially useful for long-term assessments of soil erosion with net carbon loss and carbon fate in particular sectors since, in contrast to empirical models, it provides accurate estimations (Mariappan et al., 2022). According to Stroosnijder (2005), the FRN technique is more appropriate for studying natural (geological) erosion in landscape ecology and geomorphology than it is for studying human-caused accelerated erosion. Parsons and Foster (2011) questioned the suitability of FRNs in hilly and mountainous areas with uneven soil distributions

http://www.aloki.hu ● ISSN 1589 1623 (Print) ● ISSN 1785 0037 (Online)
DOI: http://dx.doi.org/10.15666/aeer/2304_61616176

and the characteristics of bare rock outcrops. Despite this, several studies by Evrard et al. (2020), Foucher et al. (2021), and Meusburger et al. (2018) highlighted the validity and application of the FRN Caesium-137, the most widely used and reliable tracer for assessing the soil erosion rate and understanding erosion processes. The upper slope experienced greater erosion and downwards to the middle slope and lower slope, and deposition took place at the bottom of the hill slope. The observed soil redistribution patterns on terraced fields align with the erosion and deposition patterns typically associated with soil erosion, as indicated by previous studies (Meliho et al., 2019; Quine et al., 1999).

Estimation of erosion

From the highest fallout period in South America (1964–1972) to the sample date, ^{137}Cs readings are used to derive information on mean yearly erosion rates during the previous 50–60 years (Chaboche et al., 2021, 2022). The methodological recommendations for applying this approach are given by Zapata (2002), Mabit et al. (2014b) and Fulajtar et al. (2017).

We can recreate soil redistribution rates and assess the sustainability of farming techniques during the period of agricultural intensification beginning in roughly the 1960s by measuring soil inventories of ^{137}Cs (Zapata, 2003; Vanwalleghem et al., 2017). Consequently, the older erosion events that occurred shortly after ^{137}Cs fell were mostly reflected in the ^{137}Cs tracer. Recent soil loss has less of an impact on the ^{137}Cs inventories since these events occurred after a portion of the ^{137}Cs had already vanished as a result of decay and earlier erosion. Accordingly, rather than contemporary soil redistribution, ^{137}Cs inventories should be more sensitive to historical erosion events (Zhang et al., 2006; Porto et al., 2016).

In the study region, the total ^{137}Cs inventory of farmed sites was lower than the reference inventory, indicating net soil loss; however, it was greater at the bottom position, indicating sediment deposition. According to Gutierrez et al. (2015), soil loss was more noticeable on steeply sloping terraces and comparatively less noticeable on moderately sloping terraces because the rate of soil movement downslope was proportional to the slope.

To convert the FRN inventory into soil redistribution rates for ploughed and/or unploughed soils, numerous conversion models have been created (Walling et al., 2011; Arata et al., 2016; Gharbi et al., 2020). To establish FRN inventories for rates of soil erosion and sedimentation, a variety of models, ranging from straightforward empirical models to intricate mass balance models, are available (Walling et al., 2007). Mass balance models have been widely applied to ascertain the spatial distribution of rates of deposition and erosion. Because it produces physically realistic results, mass balance model II (MBM-II) is typically used to transform total FRN activities into soil redistribution rates (Zhang et al., 1999).

The redistribution of ^{137}Cs in the landscape was likely significantly influenced by topographic parameters such as slope, slope form, and aspect. The slope gradient and slope length are known to affect farmland soil erosion and runoff rates (Zhao et al., 2022). The estimated erosion/deposition soil eroded from the summit and upper slope positions by 24.93 and 6.33 t ha^{-1} yr^{-1}, respectively, and was deposited at the middle slope position (10.21 t ha^{-1} yr^{-1}), lower slope position (38.34 t ha^{-1} yr^{-1}), and bottom position (51.26 t ha^{-1} yr^{-1}). This result is similar to that of Kothyari et al. (2004), where the maximum soil erosion rate, 5.47 t ha^{-1} yr^{-1}, was recorded. According to

http://www.aloki.hu ● ISSN 1589 1623 (Print) ● ISSN 1785 0037 (Online)
DOI: http://dx.doi.org/10.15666/aeer/2304_61616176

Kalambukkattu et al. (2021), soil erosion rates in deciduous and evergreen forests range from 10 t ha^{-1} yr^{-1}. as opposed to cultivated regions. Mass balance models have been used frequently to determine the spatial patterns of erosion and deposition rates. The sediment delivery ratio was -219%, the gross erosion rate was 5.2 t ha^{-1} yr^{-1}, and the net erosion rate was 11.4 t ha^{-1} yr^{-1}. The lower elevation received soil that had eroded from the higher level.

This is because multiple calibration techniques have shown this to be the case. An erosion model's description of the processes involved in soil redistribution and erosion can be clarified with the help of the FRN. This method allows us to determine the geographical distribution of the soil erosion rate at the point scale, and it can be used as an exclusive or supplemental approach for soil erosion estimation.

Conclusion

Determining the erosion rates that occurred in the first decades following atmospheric nuclear weapon tests (1960s-1990s) is made possible via ^{137}Cs. Depending on the elevation, FRN (^{137}Cs, ^{210}Pb, ^{226}Ra, and ^{210}Pbex) was dispersed in the soil at various depths at our study site. The soil was deposited at the middle slope position (10.21 t ha^{-1} yr^{-1}), lower slope position (38.34 t ha^{-1} yr^{-1}), and bottom position (51.26 t ha^{-1} yr^{-1}) and eroded from the summit and upper slope positions by 24.93 and 6.33 t ha^{-1} yr^{-1}, respectively. The sediment delivery ratio was -219%, the gross erosion rate was 5.2 t ha^{-1} yr^{-1}, and the net erosion rate was 11.4 t ha^{-1} yr^{-1}. Our analysis also revealed that in heavily eroded farmed slopes, ^{210}Pb, ^{226}Ra, and ^{210}Pbex presented relatively high mass concentrations. The study also highlighted the necessity of thoroughly investigating the ^{137}Cs potential in the area and revealed the potential of the ^{137}Cs potential as a marker for tracking soil redistribution throughout hill slopes.

Author contributions. Mahbubur Rahmn Khan, Md. Mahbubul Alam Tarafder, Akbar Hossain: conceptualization, methodology, validation; Mahbubur Rahmn Khan, Md. Mahbubul Alam Tarafder, Ahmed Gaber, Viliam Barek, Marian Brestic, Akbar Hossain: data analysis; Mahbubur Rahmn Khan, Md. Mahbubul Alam Tarafder: original draft preparation; Ahmed Gaber, Akbar Hossain, Viliam Barek, Marian Brestic: reviewing and final editing; Mahbubur Rahmn Khan, Md. Mahbubul Alam Tarafder, Ahmed Gaber, Viliam Barek, Marian Brestic, Akbar Hossain: investigation, supervision; Mahbubur Rahmn Khan, Md. Mahbubul Alam Tarafder, Ahmed Gaber, Akbar Hossain, Viliam Barek, Marian Brestic: software, Mahbubur Rahmn Khan, Md. Mahbubul Alam Tarafder, Ahmed Gaber, Akbar Hossain: methodology; Mahbubur Rahmn Khan, Md. Mahbubul Alam Tarafder, Ahmed Gaber, Viliam Barek, Marian Brestic, Akbar Hossain: formal analysis. All authors reviewed the findings and accepted the final version of the manuscript.

Acknowledgements. All the authors are grateful to the honorable director general, BINA, along with the head of the Soil Science Division for their inspiration, financial support, and regular supervision of the study. The authors extend their appreciation to the projects of the Research and Development Support Agency APVV-15-0562 and APVV-20-0071. The authors also extend their appreciation to the Operational Program Integrated Infrastructure within the project: Demand-driven Research for the Sustainable and Innovative Food, Drive4SIFood 313011V336, cofinanced by the European Regional Development Fund. The authors also extend their appreciation to Taif University, Saudi Arabia, for supporting this work through project number TU-DSPP-2024-07.

Funding. This research was financially supported by the Bangladesh Institute of Nuclear Agriculture (BINA), Mymensingh 2202, Bangladesh. This work was also financially supported by the projects of the Research and Development Support Agency APVV-15-0562 and APVV-20-0071. This publication was also supported by the Operational Program Integrated Infrastructure within the project: Demand-driven

Research for the Sustainable and Innovative Food, Drive4SIFood 313011V336, cofinanced by the European Regional Development Fund. This research was also funded by Taif University, Saudi Arabia, Project No. (TU-DSPP-2024-07).

Conflict of interests. The authors declare that they have no competing financial interests.

Data availability statement. The datasets generated during and/or analyzed during the current study will be available from the corresponding author upon request.

REFERENCES

[1] Alewell, C., Meusburger, K., Juretzko, G., Mabit, L., Ketterer, M. E. (2014): Suitability of 239 + 240Pu and ^{137}Cs as tracers for soil erosion assessment in mountain grasslands. – Chemosphere 103: 274-280. https://doi.org/10.1016/j.chemosphere.2013.12.016.

[2] Arata, L., Meusburger, K., Frenkel, E., A'campo-Neuen, A., Iurian, A., Ketterer, M. E., Mabit, L., Alewell, C. (2016): Modelling Deposition and Erosion rates with RadioNuclides (MODERN). Part 1: A new conversion model to derive soil redistribution rates from inventories of fallout radionuclides. – Journal of Environmental Radioactivity 162-163: 45-55. https://doi.org/10.1016/j.jenvrad.2016.05.009.

[3] Blanco-Canqui, H., Lal, R. (2010): Soil and Water Conservation. – In: Blanco-Canqui, H., Lal, R. (eds.) Principles of Soil Conservation and Management. Springer, Dordrecht. https://doi.org/10.1007/978-1-4020-8709-7_1.

[4] Bujan, A., Santanatoglia, O. J., Chagas, C., Massobrio, M., Castiglioni, M., Yanez, M., Ciallella, H., Fernandez, J. (2003): Soil erosion evaluation in a small basin through the use of 137Cs technique. – Soil Tillage Research 69(1-2): 127-137. https://doi.org/10.1016/S0167-1987(02)00134-4.

[5] Chaboche, P., Pointurier, F., Sabatier, P., Foucher, A., Tiecher, T., Minella, J. P. G., Tassano, M., Hubert, A., Morera, S., Gu'Edron, S., Ardois, C. H., Boulet, B., Cossonnet, C., Cabral, P., Cabrera, M., Chalar, G., Evrard, O. (2022): ^{240}Pu/^{239}Pu signatures allow refining the chronology of radionuclide fallout in South America. – Science of the Total Environment 843: 156943. https://doi.org/10.1016/j.scitotenv.2022.156943.

[6] Chaboche, P., Saby, N. A. P., Laceby, J. P., Minella, J. P. G., Tiecher, T., Ramon, R., Tassano, M., Cabral, P., Cabrera, M., Jacques, Y., Bezerra, A., Da Silva, L., Evrard, O. (2021): Mapping the spatial distribution of global ^{137}Cs fallout in soils of South America as a baseline for earth science studies. – Earth-Science Reviews 214: 103542. https://doi.org/1016/j. earscirev.2021.103542.

[7] Collins, A. L., Walling, D. E., Sichingabula, H. M., Leeks, G. J. L. (2001): Using 137Cs measurements to quantify soil erosion and redistribution rates for areas under different land use in the Upper Kaleya River basin, southern Zambia. – Geoderma 104(3-4): 299-323. https://doi.org/10.1016/S0016-7061(01)00087-8.

[8] Dercon, G., Deckers, J., Poesen, J., Govers, G., Sánchez, H., Ramírez, M., Vanegas, R., Tacuri, E., Loaiza, G. (2006): Spatial variability in crop response under contour hedgerow systems in the Andes region of Ecuador. – Soil and Tillage Research 86(1): 15-26. https://doi.org/10.1016/j.still.2005.01.017.

[9] Dercon, G., Govers, G., Poesen, J. E. A., Sánchez, H., Rombaut, K., Vandenbroeck, E., Loaiza, G., Deckers, J. (2007): Animal-powered tillage erosion assessment in the southern Andes region of Ecuador. – Geomorphology 87(1-2): 4-15. https://doi.org/10.1016/j.geomorph.2006.06.045.

[10] Duan, X., Xie, Y., Ou, T., Lu, H. (2011): Effects of soil erosion on long-term soil productivity in the black soil region of northeastern China. – Catena 87(2): 268-275. https://doi.org/10.1016/j.catena.2011.06.012.

http://www.aloki.hu ● ISSN 1589 1623 (Print) ● ISSN 1785 0037 (Online)
DOI: http://dx.doi.org/10.15666/aeer/2304_61616176

[11] Evrard, O., Chaboche, P. A., Ramon, R., Foucher, A., Laceby, J. P. (2020): A global review of sediment source fingerprinting research incorporating fallout radiocesium (^{137}Cs). – Geomorphology 362: 107103. https://doi.org/10.1016/j.geomorph.2020.107103.
[12] FAO (2019): Outcome Document of the Global Symposium on Soil Erosion. – Food and Agriculture Organization of the United Nations, Rome.
[13] Foucher, A., Chaboche, P. A., Sabatier, P., Evrard, O. (2021): A worldwide meta-analysis (1977-2020) of sediment core dating using fallout radionuclides including ^{137} Cs and ^{210} Pbexs. – Earth System Science Data 13: 4951-4966. https://doi.org/10.5194/essd-13-4951-2021.
[14] Fulajtar, E., Mabit, L., Renschler, C. S., Lee, A., Yi, Z. (2017): Use of 137 Cs for Soil Erosion Assessment. – FAO, Rome.
[15] Gharbi, F., Alsheddi, T. H., Ben Ammar, R., Ahmed, E. N. M. (2020): Combination of ^{137}Cs and ^{210}Pb radioactive atmospheric fallouts to estimate soil erosion for the same time scalent. – Journal of Environmental Research 17(22): 8292. https://doi.org/10.3390/ijerph17228292.
[16] Gutiérrez-Girón, A., Díaz-Pinés, E., Rubio, A., Gavilán, R. G. (2015): Both altitude and vegetation affect temperature sensitivity of soil organic matter decomposition in Mediterranean high mountain soils. – Geoderma 237: 1-8. https://doi.org/10.1016/j.geoderma.2014.08.005.
[17] IAEA (2014): Guidelines for Using Fallout Radionuclides to Assess Erosion and Effectiveness of Soil Conservation Strategies. – IAEA TECDOC No., 1741(2014).
[18] Kalambukkattu, J. G., Kumar, S., Hole, R. M. (2021): Geospatial modelling of soil erosion and risk assessment in Indian Himalayan region—a study of Uttarakhand state. – Environmental Advances 4: 100039. https://doi.org/10.1016/j.envadv.2021.100039.
[19] Konz, N., Prasuhn, V., Alewell, C. (2012): On the measurement of alpine soil erosion. – Catena 91: 63-71. https://doi.org/10.1016/j.catena.2011.09.010.
[20] Kothyari, B. P., Verma, P. K., Joshi, B. K., Kothyari, U. C. (2004): Rainfall–runoff-soil and nutrient loss relationships for plot size areas of Bhetagad watershed in Central Himalaya, India. – Journal of Hydrology 293(1-4): 137-50. https://doi.org/10.1016/j.jhydrol.2004.01.011.
[21] Kumar, S., Raj, A. D., Kalambukkattu, J. G. (2023): Geospatial Modelling for Sustainability of Soil Ecosystem Services in Hilly and Mountainous Landscapes. – In: Chatterjee, U. et al. (eds.) Water, Land, and Forest Susceptibility and Sustainability. Academic Press, Cambridge, MA, pp. 331-359. https://doi.org/10.1016/B978-0-443-15847-6.00011-2.
[22] Mabit, L., Benmansour, M., Walling, D. E. (2008): Comparative advantages and limitations of the fallout radionuclides ^{137}Cs, ^{210}Pbex and ^{7}Be for assessing soil erosion and sedimentation. – Journal of Environmental Radioactivity 99(12): 1799-1807. https://doi.org/10.1016/j.jenvrad.2008.08.009.
[23] Mabit, L., Meusburger, K., Fulajitar, E., Alewell, C. (2013): The usefulness of ^{137}Cs as a tracer for soil erosion assessment: a critical reply to parsons and foster. – Earth-Science Reviews 137: 300-307. https://doi.org/10.1016/j.earscirev.2013.05.008.
[24] Mabit, L., Benmansour, M., Abril, J. M., Walling, D. E., Meusburger, K., Iurian, A. R., Alewell, C. (2014a): Fallout 210Pb as a soil and sediment tracer in catchment sediment budget investigations: a review. – Earth-Science Reviews 138: 335-351. https://doi.org 10.1016/j.earscirev.2014.06.007.
[25] Mabit, L., Chem-Kieth, S., Dornhofer, P., Toloza, A. (2014b): ^{137}Cs: A widely used and validated medium term soil tracer. Guidelines for using fallout radionuclides to assess erosion and effectiveness of soil conservation strategies. – IAEA TECDOC-1741, pp. 27-77. http://www-pub.iaea.org/MTCD/Publications/PDF/TE-1741_web.pdf.
[26] Mandal, D., Giri, N., Srivastava, P., Sah, C., Bhusan, R., Naregundi, K., Mohan, M. P., Shrivastava, M. (2019): ^{137}Cs—a potential environmental marker for assessing erosion-

http://www.aloki.hu ● ISSN 1589 1623 (Print) ● ISSN 1785 0037 (Online)
DOI: http://dx.doi.org/10.15666/aeer/2304_61616176

induced soil organic carbon loss in India. – Current Science 117(5): 865-871. http://dx.doi.org/10.18520/cs/v117/i5/865-871.
[27] Mariappan, S., Hartley, I. P., Cressey, E. L., Dungait, J. A., Quine, T. A. (2022): Soil burial reduces decomposition and offsets erosion-induced soil carbon losses in the Indian Himalaya. – Global Change Biology 28(4): 1643-1658. https://doi.org/10.1111/gcb.15987.
[28] Meliho, M., Nouira, A., Benmansour, M., Boulmane, M., Khattabi, A., Mhammdi, N., Benkdad, A. (2019): Assessment of soil erosion rates in a Mediterranean cultivated and uncultivated soils using fallout ^{137}Cs. – Journal of Environmental Radioactivity 208: 106021. https://doi.org/10.1016/j.jenvrad.2019.106021.
[29] Meusburger, K., Porto, P., Mabit, L., La Spada, C., Arata, L., Alewell, C. (2018): Excess Lead-210 and Plutonium-239 + 240: two suitable radiogenic soil erosion tracers for mountain grassland sites. – Environmental Research 160: 195-202. https://doi.org/10.1016/j.envres.2017.09.020.
[30] Porto, P., Walling, D. E., Cogliandro, V., Callegari, G. (2016): Exploring the potential for using 210Pbex measurements within a resampling approach to document recent changes in soil redistribution rates within a small catchment in southern Italy. – Journal of Environmental Radioactivity 164: 158-168. https://doi.org/10.1016/j.jenvrad.2016.06.026.
[31] Quine, T. A., Walling, D. E., Chakela, Q. K., Mandiringana, O. T., Zhang, X. (1999): Rates and patterns of tillage and water erosion on terraces and contour strips: evidence from caesium-137 measurements. – Catena 36(1-2): 115-42. https://doi.org/10.1016/S0341-8162(99)00006-5.
[32] Ritchie, J. C., Ritchie, C. A. (2001): Bibliography of publication of Cesium-137 studies related to erosion and sediment deposition. – USDA-ARS Hydrology and Remote sensing Laboratory, Beltsville, MD.
[33] Schmitter, P., Dercon, G., Hilger, T., Le Ha, T. T., Thanh, N. H., Lam, N., Vien, T. D., Cadisch, G. (2010): Sediment induced soil spatial variation in paddy fields of Northwest Vietnam. – Geoderma 155(3-4): 298-307. https://doi.org/10.1016/j.geoderma.2009.12.014.
[34] Tagami, K., Tsukada, H., Uchida, S. (2019): Quantifying spatial distribution of ^{137}Cs in reference site soil in Asia. – Catena 180: 341-345. https://doi.org/10.1016/j.catena.2019.05.009.
[35] Van Oost, K., Six, J. (2023): Reconciling the paradox of soil organic carbon erosion by water. – Biogeosciences 20(3): 635-646. https://doi.org/10.5194/bg-20-635-2023.
[36] Vanwalleghem, T., Gómez, J. A., Amate, J. I., De Molina, M. G., Vanderlinden, K., Guzmán, G., Laguna, A., Giráldez, J. V. (2017): Impact of historical land use and soil management change on soil erosion and agricultural sustainability during the Anthropocene. – Anthropocene17: 13-29. https://doi.org/10.1016/j.ancene.2017.01.002.
[37] Walling, D. E., He, Q. (1997): Models of Converting ^{137}Cs Measurements to Estimates of Soil Redistribution Rates on Cultivated and Uncultivated Soils (Including Software for Model Implementation). – Report to IAEA. University of Exeter, pp. 315-341.
[38] Walling, D. E., Quine, T. (1993): Use of Caesium-137 as a Tracer of Erosion and Sedimentation: Handbook for the Application of the ^{137}Cs Technique. – University of Exeter, Department of Geography, Exeter.
[39] Walling, D. E., Zhang, Y., He, Q. (2007): Models for Converting Measurements of Environmental Radionuclide Inventories (^{137}Cs, Excess ^{210}Pb and ^{7}Be) to Estimates of Soil Erosion and Deposition Rates (Including Software for Model Implementation). – University of Exeter, Department of Geography, Exeter.
[40] Walling, D., Zhang, Y., He, Q. (2011): Models for deriving estimates of erosion and deposition rates from fallout radionuclide (caesium-137, excess lead-210, and beryllium-7 measurements the development of user-friendly software for model implementation.

http://www.aloki.hu ● ISSN 1589 1623 (Print) ● ISSN 1785 0037 (Online)
DOI: http://dx.doi.org/10.15666/aeer/2304_61616176

Impact of soil conservation measures on erosion control and soil quality. – IAEA-TECDOC-1665: 11-33.
[41] Walling, D. E., Porto, P., Zhang, Y., Du, P. (2014): Upscaling the use of fallout radionuclides in soil erosion and sediment budget investigations: addressing the challenge. – International Soil and Water Conservation Research 2(3): 1-21. https://doi.org/10.1016/S2095-6339(15)30019-8.
[42] Zapata, F. (2002): Handbook for the Assessment of Soil Erosion and Sedimentation Using Environmental Radionuclides. – Springer, Dordrecht. https://doi.org/10.1007/0-306-48054-9.
[43] Zapata, F. (2003): The use of environmental radionuclides as tracers in soil erosion and sedimentation investigations: recent advances and future developments. – Soil Tillage Research 69(1-2): 3-13. https://doi.org/10.1016/S0167-1987(02)00124-1.
[44] Zhang, F., Wang, J., Du, J. (2021): A global dataset of atmospheric ^{7}Be and ^{210}Pb measurements: annual air concentration and depositional flux. – Earth System Science Data 13: 2963-2994. https://doi.org/10.5194/essd-13-2963-2021.
[45] Zhang, X., Qi, Y., Walling, D. E., He, X., Wen, A., Fu, J. (2006): A preliminary assessment of the potential for using ^{210}Pbex measurement to estimate soil redistribution rates on cultivated slopes in the Sichuan Hilly Basin of China. – Catena 68(1): 1-9. https://doi.org/10.1016/j.catena.2006.03.012.
[46] Zhang, X. B., Walling, D. F., He, Q. (1999): Simplified mass balance models for assessing soil erosion rates on cultivated land using caesium-137 measurements. – Hydrological Sciences Journal 44(1): 33-45. https://doi.org/10.1080/02626669909492201.
[47] Zhao, J., Wang, Z., Dong, Y., Yang, Z., Govers, G. (2022): How soil erosion and runoff are related to land use, topography and annual precipitation: insights from a meta-analysis of erosion plots in China. – Science of the Total Environment 802: 149665. https://doi.org/10.1016/j.scitotenv.2021.149665.